Investigation of the photosynthetic response of Chlorella vulgaris to light changes in a torus-shape photobioreactor

M Bonnanfant, Hélène Marec, Bruno Jesus, Jean-Luc Mouget, Jeremy Pruvost

Investigation of the photosynthetic response of *Chlorella vulgaris* to light changes in a torus-shape photobioreactor

M. Bonnanfant[1,2] · H. Marec[1] · B. Jesus[3] · J.-L. Mouget[2] · J. Pruvost[1]

Abstract
An efficient use of light is essential to achieve good performances in microalgae cultivation systems. This can be challenging particularly under solar conditions where light is highly dynamic (e.g., day/night cycles, rapid changes in wind and weather conditions). Microalgae display different mechanisms to optimize light use efficiency. In the short term, when high light is encountered, several processes of photoprotection can be involved to avoid cell damages (e.g., xanthophyll cycle). In the long term, when cells are exposed to a different light intensity, pigment content changes, i.e., photoacclimation. The purpose of this study is to investigate the photosynthetic response of *Chlorella vulgaris* cultures grown in closed lab-scale, torus-shape photobioreactor under well-controlled light conditions, namely, constant and dynamic light transitions. Experiments were conducted in continuous mode with detailed characterization of the light attenuation conditions for each condition, as represented by the mean rate of photon absorption (MRPA), so as to characterize the time responses of the photosynthetic cells toward light changes. This enables to observe short-term and long-term responses with their own characteristic times. The mechanisms involved were found to be different between increasing and decreasing light transitions. Furthermore the MRPA was found a valuable parameter to relate the effect of light to biological responses (i.e., pigment changes) under constant light and dynamic light conditions.

Key points
- *MRPA proved valuable to relate C. vulgaris responses to light changes.*
- *A linear evolution was found between pigment content and MRPA in continuous light.*
- *A rising PFD step induced fast protection and acclimation mechanisms.*

Keywords Microalgae · Light response · Photosynthesis · Photoacclimation · Photoprotection

Introduction

An efficient use of light is essential to achieve good performances in microalgae production, particularly in mass cultivation systems under solar conditions where light is highly dynamic (Richmond 2013). These light variations are mainly due to the diurnal cycles during which the incident photon flux density (PFD or q_0) is changing from null to very high values, greater than 1200 $\mu mol_{photons}\ m^{-2}\ s^{-1}$ in summer in Western France (Le Borgne 2011).

In order to avoid contaminations by bacteria, fungus, or other microalgal cells, microalgae are often cultivated in closed photobioreactors (PBRs). Controlling culture conditions prevents growth limitation due to pH, temperature, or culture medium variations (Pruvost et al. 2016). As a result, light can become the main limiting parameter for the maximization of growth kinetics and biomass productivity. Light-use optimization is however complex, with the distribution of light in the culture medium being heterogeneous. Due to the cells in suspension and photosynthesis, light is absorbed, creating a gradient of light level along the culture depth (Pruvost et al. 2008). Depending on external conditions such as PFD and dilution rate, even when the PFD applied onto the PBR is the same, the light attenuation profile, and thus light regimes into the culture medium, can be very different.

✉ J. Pruvost
jeremy.pruvost@univ-nantes.fr

[1] GEPEA, UMR 6144, Oniris, CNRS, Université de Nantes, 44600 Saint-Nazaire, France

[2] Mer-Molécules-Santé (MMS), EA 2160, Le Mans Université, Le Mans Cedex 9, France

[3] Mer-Molécules-Santé (MMS), EA2160, Faculté Des Sciences, Université de Nantes, Nantes, France

Microalgal cells absorb light energy through light harvesting complexes and use that energy for carbon fixation through photosynthesis (Crofts and Wraight 1983). However, if the light energy is excessive, the photosynthetic apparatus becomes overexcited and harmful reactive oxygen species (ROS) are produced (Muller et al. 2001). In some cases, it results in cell photoinhibition leading to a loss of biomass productivity (Kok 1956; Nixon et al. 2010). On the contrary, if light energy is too low, other mechanisms such as respiration occur in the PBR, also leading to productivity loss (Bennoun 1982; Peltier and Cournac 2002).

To prevent these phenomena, microalgae have mechanisms to optimize the efficiency of their light utilization. In the short term, when excessive light is encountered, they can activate several photoprotection processes to avoid cell damages (Prasil et al. 1996; Asada 2000; Lavaud 2007; Kargul and Barber 2008). Among them, the non-photochemical fluorescence quenching (NPQ) is an important mechanism, which allows microalgae to quickly respond to a rapid increase in light received and avoid photo-damage. The major component of this process is due to the de-epoxidation of some xanthophylls, resulting in the dissipation as heat of the excess light energy, which cannot be used for photosynthesis (Goss and Lepetit 2015).

In a longer time scale, when cells are exposed to a different light intensity, their pigment content is also known to change within a process named photoacclimation. When cells are exposed to low light, their pigment content per cell increases, which increases cell absorption capacity. On the contrary, when cells are exposed to high light, their pigment content decreases to reduce the production of ROS and the oversaturation effect (Dubinsky and Stambler 2009).

In PBRs, the overall pigment concentration has a direct impact on the light transfer and therefore on the photosynthetic growth rate, and thus on the resulting PBR biomass productivity. So photoacclimation processes can influence the reactor performances (Pruvost et al. 2015).

The purpose of this study is to investigate the photoacclimation of *Chlorella vulgaris* cultures grown in a closed lab-scale PBR under well-controlled conditions of light received. First, the changes in the cellular pigment content due to photoacclimation will be studied in PBR operating at constant light. Then the dynamics of the acclimation processes will be examined during light step transitions.

Material and methods

Pre-culture protocol

The strain *Chlorella vulgaris* CCAP 21.119 was grown in a modified Bold's basal medium (BBM) in 250-mL Erlenmeyer flasks under 60 $\mu mol_{photons}\ m^{-2}\ s^{-1}$ (Andersen 2005). The culture was continuously stirred. Algae were sub-cultured every 2 weeks; 1 mL from old culture was inoculated in 100 mL of new fresh BBM (Kazbar et al. 2019b).

Culture protocol

Cultivation system

Experiments were conducted in a laboratory-scale PBR of torus shape presenting a flat illuminated surface, a square-channel (i.e., Cartesian geometry for light attenuation) and a depth of culture of 0.04 m (i.e., perpendicular to illuminated surface) for a total culture volume of 1.5 L (Fig. 1). A complete description can be found in Pruvost et al. (2006). The interest of this system to control with a high accuracy all culture parameters influencing photosynthesis and growth has already been demonstrated in several works (Pottier et al. 2005; Degrenne et al. 2010; Takache et al. 2015; Souliès et al. 2016; Kazbar et al. 2019a).

To avoid any bias due to cell acclimation (as usually observed after inoculation), all cultures were carried out in continuous chemostat mode, with continuous addition of fresh culture medium. The flowrate was adjusted depending of the targeted dilution rate. Sufficient culture duration in constant conditions (i.e., usually several days) was applied to allow the culture to stabilize to the light conditions imposed.

The artificial incident PFD was provided by a panel of white light LEDs. The light from the LED panel was calibrated with a quantum sensor (Li-COR 250A, USA). Agitation was mainly provided by a marine impeller. During experiments, the temperature was maintained at 25 °C by automatic water cooling, the pH was monitored (InPro 3253i Mettler Toledo, USA) and maintained at 7.5 by automatic CO_2 injection, and the dissolved oxygen concentration was measured (InPro 6860i Mettler Toledo, USA) and controlled by automatic N_2 bubbling for degassing. Both pH and oxygen concentrations were regulated with a proportional integral derivative (PID) controller (Ifrim et al. 2014; Titica et al. 2018). All regulations were done using Labview software (Laboratory Virtual Instrument Engineering Workbench, National Instrument, USA). Data were recorded in real time.

For these experiments, *C. vulgaris* cultures were carried out in Sueoka medium (i.e., with ammonium as the nitrogen source) supplemented with Hutner solution (Sueoka 1960; Souliès et al. 2016). The concentration of nutrients was adjusted to be in excess, so that microalgae growth was only light-limited (Souliès et al. 2016; Kazbar et al. 2019a).

Culture conditions in constant light

In order to investigate *C. vulgaris* photoacclimation in constant light regime, several cultures were carried out

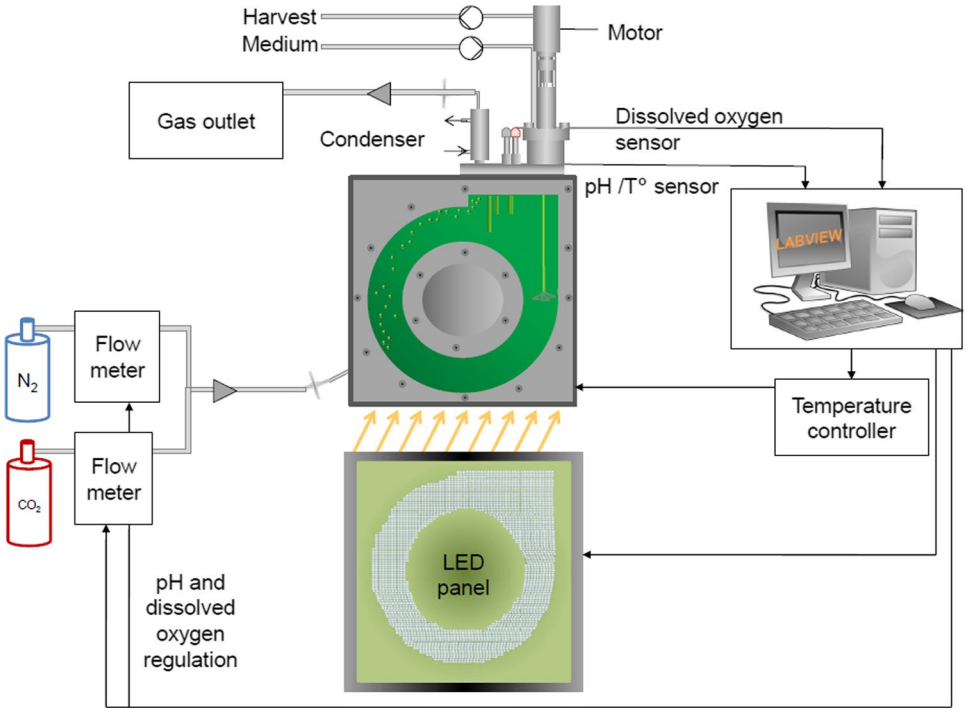

Fig. 1 Controlled photobioreactor used for the study of the photosynthetic response of *C. vulgaris*

in continuous mode (Table 1). The imposed PFD ranged between 50 and 800 $\mu mol_{photons}\ m^{-2}\ s^{-1}$ and the imposed dilution rate D ranged between 0.01 and 0.07 h^{-1}.

For each condition, the culture was carried out in the PBR for at least 5 resident times until obtaining a steady-state (i.e., constant biomass and pigment concentrations). When steady-state was reached, 30 to 50 mL of culture was sampled for analyses. Samplings were done in triplicate in order to validate the steady-state regime.

Incident light transitions

To study *C. vulgaris* photoacclimation under dynamic light, two successive light step transitions in incident PFD were done (Fig. 2). Instead of light cycles, the choice of applying light transitions was made to allow the measurement of characteristic times after a single increasing or decreasing light change. A large amplitude between the two PFD levels was chosen to facilitate the observations.

A first, steady-state was reached for an incident PFD equal to 75 $\mu mol_{photons}\ m^{-2}\ s^{-1}$, and then the light was changed to 765 $\mu mol_{photons}\ m^{-2}\ s^{-1}$. When the second steady-state was reached, the incident PFD was reduced back to 75

Table 1 Investigation of photoacclimation of *C. vulgaris* in constant light. Culture conditions (photon flux densities, PFD and dilution rates, D) and results obtained at steady-states (biomass concentrations, C_x; pigment concentrations, C_{pig}; illuminated fractions, γ; and transmittances obtained, T). Errors are standard deviations ($n=3$). A transmittance T equals to 0 means that all light is absorbed by the culture and then no light pass through the culture

Condition no	PFD ($\mu mol_{photons}\ m^{-2}\ s^{-1}$)	Dilution rate, D (h^{-1})	C_x ($g\ L^{-1}$)	C_{pig} ($mg\ L^{-1}$)	Illuminated fraction, γ	Transmittance, T
1	50	0.01	0.40 ± 0.02	29.2 ± 0.8	0.31	0
2	50	0.02	0.17 ± 0.00	13.7 ± 0.3	0.84	0
3	100	0.02	0.41 ± 0.02	30.1 ± 0.8	0.52	0
4	100	0.05	0.18 ± 0.03	11.7 ± 2.0	> 1	0.43
5	250	0.02	0.67 ± 0.07	40.3 ± 4.8	0.60	0
6	250	0.05	0.37 ± 0.02	18.4 ± 1.1	> 1	0.25
7	400	0.02	1.21 ± 0.04	78.7 ± 1.0	0.41	0
8	400	0.07	0.32 ± 0.04	14.0 ± 1.7	> 1	0.33
9	800	0.02	1.33 ± 0.08	66.9 ± 7.1	0.58	0
10	800	0.01	1.80 ± 0.04	105.6 ± 1.2	0.40	0
11	800	0.04	1.01 ± 0.01	49.9 ± 1.9	0.80	0

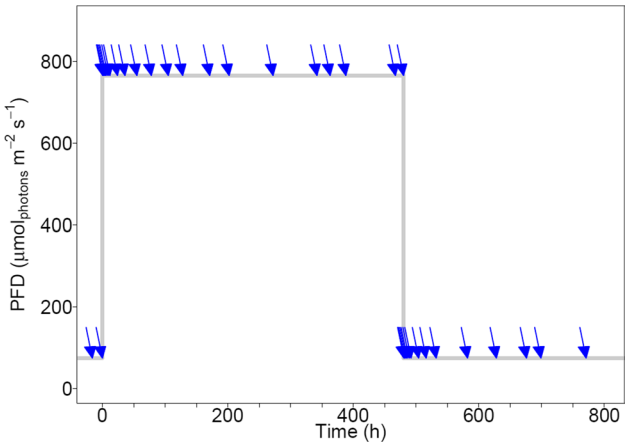

Fig. 2 PFD step transitions applied during the investigation of photoacclimation of *C. vulgaris* in light changing conditions. Arrows show sampling times

$\mu mol_{photons}\ m^{-2}\ s^{-1}$ until the third steady-state was reached. The dilution rate (D) was constant at 0.02 h^{-1} during the whole experiment.

Immediately after each PFD step, several culture samples were regularly taken and the sampling was less frequent over time thereafter. For each sample, about 30 mL of culture was taken. After each sampling, the harvest pump was stopped until the culture volume reached its pre-sampling value.

Analyses

PAM chlorophyll a fluorescence parameters

To measure photosynthetic parameters, off-line PAM chlorophyll *a* measurements were done using a PAM fluorometer (WaterPAM, Walz, Germany). Immediately after each sampling, cultures were diluted in Sueoka medium in a quartz cuvette so that the fluorescence signal was close to 200 units (Heinz Walz GmbH 2001). The dilution mainly depended on the chlorophyll *a* concentration. The culture was left for 10 to15 min in darkness in order to allow the total oxidation of PSII reaction centers.

After dark acclimation, a rapid light curve (RLC) was carried on the samples (Perkins et al. 2010) with 8 incremental light levels, i.e., 0, 75, 109, 165, 245, 346, 479, 773, and 1127 $\mu mol_{photons}\ m^{-2}\ s^{-1}$. After 1.5-min exposure to each light level, a saturating flash was applied for 0.8 s to close all open PSII reaction centers. After each light level, the following parameters were measured: F', F_m', F_o (at the 1st measurement), F_m (at the 1st measurement).

Maximum PSII quantum yield for photochemical energy conversion (F_v/F_m) was calculated as follows (Kolber and Falkowski 1993):

$$F_v/F_m = \frac{F_m - F_o}{F_m} \quad (1)$$

PSII quantum yield of regulated non-photochemical energy loss ($YNPQ$) was calculated as follows (Klughammer and Schreiber 2008):

$$YNPQ = \frac{F}{F_m'} - \frac{F}{F_m} \quad (2)$$

In Eq. 2, F_m' was the value measured for the actinic light equal to the average fluence rate of the culture (G_{mean}, see next).

Biomass concentration

Microalgae biomass concentration was determined based on dry matter measurement (g L^{-1}). Depending on the microalgae concentration, a known volume of culture (between 6 and 15 mL) was filtered on a pre-weighted dry glass microfiber filter with a pore size of 0.7 µm. Then the filters were dried at 105 °C. At least 24 h later, the filters were cooled in a desiccator and weighted again.

Pigment concentration

Depending on the culture concentration, a known volume (V_{samp}) of culture (between 0.1 to 2 mL) was centrifuged for 10 min at 13,400 g (MiniSpin Eppendorf, Germany). Supernatant was removed and the pellet was re-suspended in 1.5 mL of methanol. The tubes were left for 45 min at 45 °C to allow the extraction of pigments in methanol. After centrifugation, a white pellet was obtained, which proved the total extraction of the pigments. The absorbance was measured with a spectrophotometer (Jasco V-630, France) at 430 nm, 652 nm, 665 nm, and 750 nm. The following equations were used to estimate the concentrations of chlorophyll *a*, chlorophyll *b*, and total carotenoids (Strickland and Parsons 1968; Ritchie 2008):

$$[\text{Chlorophyll } a] = \frac{1.5}{V_{samp}}\left(-8.0962 \times A_{652} + 16.5169 \times A_{665}\right) \quad (3)$$

$$[\text{Chlorophyll } b] = \frac{1.5}{V_{samp}}\left(27.4405 \times A_{652} + 12.1688 \times A_{665}\right) \quad (4)$$

$$[\text{Total carotenoids}] = \frac{1.5}{V_{samp}}\left(4 \times A_{480}\right) \quad (5)$$

with A_{652} the absorbance at 652 nm, A_{665} the absorbance at 665 nm, and A_{480} the absorbance at 480 nm.

Total pigment concentration (C_{pig} in g L^{-1}) was calculated by adding these different concentrations together. The

total pigment (w_{pig}), chlorophyll *a* (w_{Chla}), chlorophyll *b* (w_{Chlb}), and total carotenoid (w_{car}) contents were calculated by dividing the pigment concentrations by the dry biomass concentration.

Inorganic carbon concentration

Inorganic carbon concentration was measured on some samples to check that the dissolved carbon concentration was not in a limiting concentration (i.e., inferior to 5 mM (Le Gouic et al. 2021)). For that purpose, 15 mL of culture was centrifuged at 4150 g (Hettich Mikro 22R, Germany) for 10 min. Then, the supernatant was filtered and inorganic carbon concentration was measured with a carbon analyzer (TOC-L, Shimadzu, Japan).

Determination of the light attenuation conditions

Radiative transfer modeling

A two-flux model was used to determine the spectral value of the fluence rate $G_\lambda(z)$ (in $\mu mol_{photons}\ m^{-2}\ s^{-1}$) in the PBR (Pottier et al. 2005). Spectrally averaged fluence rate G_{mean} was calculated by integrating $G_\lambda(z)$ over the photosynthetically active radiation (*PAR*) and over the culture volume.

The biomass specific rate of photon absorption A_{Cx} (in $\mu mol_{photons}\ kg_{Cx}{}^{-1}\ s^{-1}$) was obtained by integrating the product of G_λ with the mass absorption coefficient Ea_λ of *C. vulgaris* over the *PAR* (Souliès et al. 2016):

$$A_{Cx} = \int_{PAR} Ea_\lambda G_\lambda d\lambda. \tag{6}$$

By integrating A_{Cx} over the culture volume, the mean biomass specific rate of photon absorption ($MRPA_{Cx}$) was determined. The radiative properties of *C. vulgaris*, necessary for this model, were obtained from Kandilian et al. (2016) and are given as supplementary materials.

In the present study, the specific mean rate of photon absorption was also expressed per unit of total pigment ($MRPA_{pig}$, in $\mu mol_{photons}\ kg_{pig}{}^{-1}\ s^{-1}$). It was calculated by dividing $MRPA_{Cx}$ by the total pigment content w_{pig}.

Light attenuation profile

For any microalgal species, a rate of photon absorption at which photosynthesis compensates for respiration can be defined (i.e., compensation point). This rate of photon absorption is named A_C, and it was estimated equal to 2800 $\mu mol_{photons}\ kg_{Cx}{}^{-1}\ s^{-1}$ in *C. vulgaris* (Souliès et al. 2016).

In the PBR used for the experiments, the light attenuation is one-dimensional (Pottier et al. 2005). In this case, an illuminated fraction can be defined and is equal to:

$$\gamma = \frac{V_{light}}{V_{PBR}} = \frac{z(A_C)}{L} \tag{7}$$

where V_{light} is the light volume of the PBR (i.e., where $A_{Cx} > A_C$), V_{PBR} is the volume of the whole PBR, $z(A_C)$ is the depth where A_C is reached, and L the thickness of the PBR.

When γ is inferior to 1, there is a dark volume, and when γ is superior to 1, the culture volume is fully illuminated without dark volume (Pruvost and Cornet, 2012). For $\gamma > 1$ conditions, the transmittance T was also calculated, to estimate the fraction of the incident PFD passing through the reactor depth:

$$T = \frac{G(z = L)}{q_0} \tag{8}$$

Results

Cultures in continuous light

Table 1 summarizes the values of biomass and pigment concentrations obtained at steady-states for the different cultures conditions. For each steady-state, light transfer conditions through radiative transfer modeling and corresponding MRPA values were calculated from Eq. 6. According to the PFD and dilution rate conditions, either diluted ($\gamma > 1$) or concentrated ($\gamma < 1$) cultures were obtained. The illuminated fraction γ was calculated for concentrated cultures and the transmittance T was calculated for diluted cultures. Figure 3 illustrates the pigment content obtained for each steady-state as a function of the $MRPA_{Cx}$ (Fig. 3a) and $MRPA_{pig}$ values (Fig. 3b). The illuminated fraction γ and the transmittance T are also given in Fig. 3.

The pigment content decreased with MRPA values (for both $MRPA_{Cx}$ and $MRPA_{pig}$). This can be approximated by two linear relations (minimum value of R^2 of 0.89), with a higher decrease for $MRPA_{Cx}$ values between 5 and 15 $\mu mol_{photons}\ g^{-1}\ s^{-1}$, followed by a small evolution for values over 15 $\mu mol_{photons}\ g^{-1}\ s^{-1}$. For the largest values of $MRPA_{Cx}$, an asymptotic behavior was observed, as the pigment content never decreased under $4\%_{Cx}$. This corresponded to an $MRPA_{Cx}$ about 25 $\mu mol_{photons}\ g^{-1}{}_{Cx}\ s^{-1}$ (0.58 $\mu mol_{photons}\ mg_{pig}{}^{-1}\ s^{-1}$), which was reached for an incident PFD equal to 400 $\mu mol_{photons}\ m^{-2}\ s^{-1}$ and a dilution rate equal to 0.07 h^{-1}. The resulting biomass concentration was 0.323 $g\ L^{-1}$.

Those linear evolutions were observed whatever the light attenuation condition (Fig. 3). For example, a concentrated culture with γ equal to 0.40 revealed the same $MRPA_{Cx}$ as a diluted culture with $\gamma > 1$ and T equal to 0.43. Both cultures exhibited same pigment content, about $6\%_{Cx}$. Note that the diluted culture ($T = 0.43$) was obtained for an incident PFD

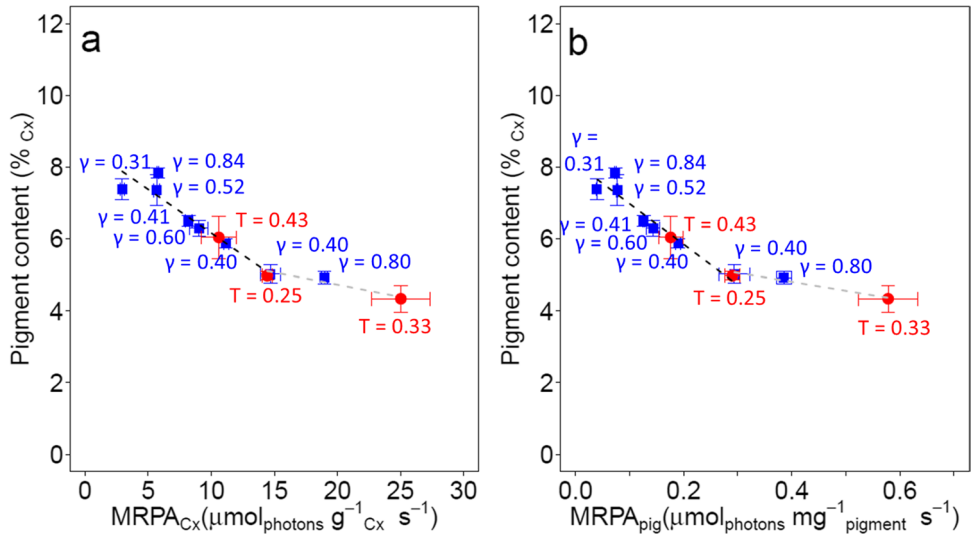

Fig. 3 Pigment content obtained for each steady-state, as a function of the $MRPA_{Cx}$ values (**a**) or the $MRPA_{pig}$ values (**b**), in diluted (red circles) and concentrated (blue squares) cultures of *C. vulgaris*. Error bars show standard deviations ($n=3$). Linear regressions were calculated (dashed line). For values of $MRPA_{Cx}$ between 3 and 14 $\mu mol_{photons}\ g^{-1}_{Cx}\ s^{-1}$ (**a**, black line), the equation is $y=8.6009-0.2436x$ and $R^2=0.89$. For values of $MRPA_{Cx}$ between 14 and 25 $\mu mol_{photons}\ g^{-1}_{Cx}\ s^{-1}$ (**a**, gray line), the equation is $y=6.089-0.0679x$ and $R^2=0.92$. For values of $MRPA_{pig}$ between 0.04 and 0.29 $\mu mol_{photons}\ mg^{-1}_{pigments}\ s^{-1}$ (**b**, black line), the equation is $y=8.1159-11.321x$ and $R^2=0.92$. For values of $MRPA_{pig}$ between 0.29 and 0.58 $\mu mol_{photons}\ mg^{-1}_{pigments}\ s^{-1}$ (**b**, gray line), the equation is $y=5.804-2.488x$ and $R^2=0.96$

equal to 100 $\mu mol_{photons}\ m^{-2}\ s^{-1}$ and a 0.05 h^{-1} dilution rate, resulting in a biomass concentration of 0.179 g L^{-1}. The concentrated culture ($\gamma=0.40$) was obtained for an incident PFD equal to 800 $\mu mol_{photons}\ m^{-2}\ s^{-1}$ and a 0.02 h^{-2} dilution rate, resulting in a biomass concentration of 1.796 g L^{-1}. Very different biomass concentrations were then achieved in both cases. A similar observation can be made for the $MRPA_{Cx}$ values at 15 $\mu mol_{photons}\ g^{-1}_{Cx}\ s^{-1}$, with two different light attenuation conditions ($T=0.25$ and $\gamma=0.40$) resulting in the same pigment content (5.0%$_{Cx}$).

Culture in dynamic light conditions

Biomass concentration and pigment content

Figure 4a shows the changes in biomass concentration and total pigment content during the two successive light step transitions. After the first PFD change from 75 to 765 $\mu mol_{photons}\ m^{-2}\ s^{-1}$, the biomass concentration needed between 150 and 200 h to almost stabilize around 1.45 ($\pm$0.12, $n=12$) g L^{-1}. Pigment content in biomass reached its lowest value of 4.5%$_{Cx}$ in the first 12 h and then it increased to reach 5.6 ($\pm$0.2, $n=9$) %$_{Cx}$ after 100 to 150 h. The culture at 765 $\mu mol_{photons}\ m^{-2}\ s^{-1}$ was highly unstable (i.e., biomass concentration and pigment content not constant), making difficult to define a precise time for the stabilization of biomass concentration. Nevertheless, it seemed that the increase in biomass concentration took more time than the decrease even if the rate for biomass increase during the first 12 h (0.026 g $L^{-1}\ h^{-1}$) was higher than the decrease (0.013 g $L^{-1}\ h^{-1}$). Instability of the culture at 765 $\mu mol_{photons}\ m^{-2}\ s^{-1}$ was probably due to both high value of dissolved oxygen concentration (around 250% of saturation) and strong agitation (50 to 100 $mL_{(N2)}\ min^{-1}$) to maintain this concentration. It must be noticed that a stronger agitation would have led to a risk of CO_2 limitation due to high degassing (Kazbar et al. 2019a).

When the PFD decreased from 765 to 75 $\mu mol_{photons}\ m^{-2}\ s^{-1}$, pigment content took about 100 h to reach a stable value around 7.9 ($\pm$0.1, $n=5$) %$_{Cx}$, which represents an increase of ca. 40%. The biomass concentration exhibited again a longer stabilization time, ca. 150 h, to reach a biomass concentration of 0.34 ($\pm$0.01, $n=4$) g L^{-1}. At the end of the experiment, at steady-state, biomass concentration and pigment content reached the same values as at the beginning of the experiment before the first light change.

Figure 4b shows the pigment composition (wt% of chlorophylls or carotenoids per total pigment) during the two successive light transitions. The composition was identical during the whole experiment, with chlorophyll *a*, chlorophyll *b*, and carotenoids representing respectively 67 $\pm$ 0.5 ($n=42$) wt%, 16 $\pm$ 0.6 ($n=42$) wt%, and 17 $\pm$ 0.4 wt% ($n=42$) of the total pigment (the error is the standard deviation calculated on *n* measurements). We can thus conclude that even if the total pigment content changed a lot (from 5.6 to 7.9%$_{Cx}$ corresponding to a 40% increase) during the successive light

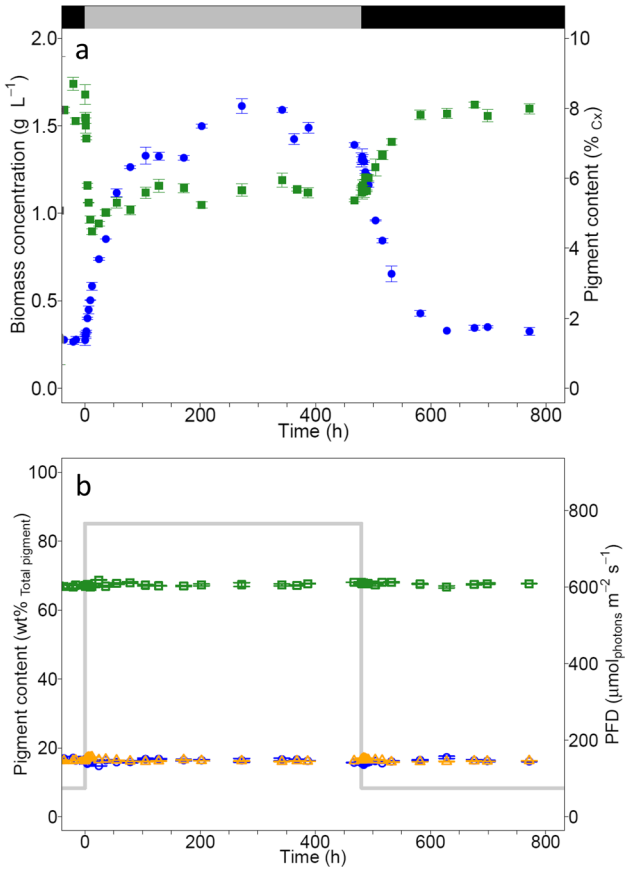

Fig. 4 Time response of *C. vulgaris* culture during a PFD step from 75 to 765 µmol$_{photons}$ m^{-2} s^{-1}, then from 765 to 75 µmol$_{photons}$ m^{-2} s^{-1}. $D=0.02$ h^{-1}. **a** shows biomass concentration (blue circles, left axis) and pigment content (green squares, right axis). Black line represents 75 µmol$_{photons}$ m^{-2} s^{-1} and gray line presents 765 µmol$_{photons}$ m^{-2} s^{-1}. **b** shows pigment compositions (green squares correspond to chlorophyll *a* content, blue circles to chlorophyll *b* content and orange triangles to total carotenoids). The gray line (right axis) represents the PFD. Error bars represent standard deviations ($n=3$)

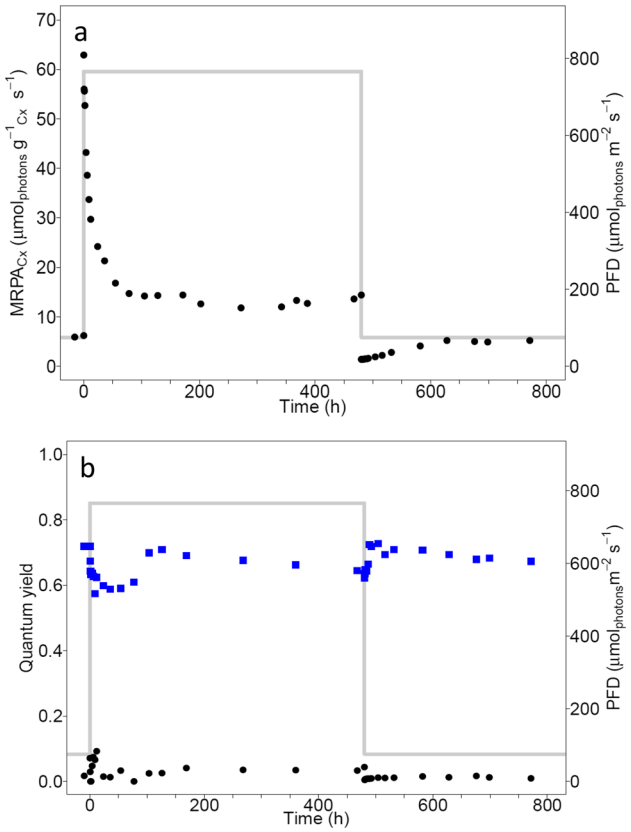

Fig. 5 Evolution with time of the $MRPA_{Cx}$ values (**a**; black circles, left axis) and of F_v/F_m and *YNPQ* (**b**; blue squares and black circles respectively, left axis) during the PFD steps from 75 to 765 µmol$_{photons}$ m^{-2} s^{-1} and from 765 to 75 µmol$_{photons}$ m^{-2} s^{-1} (gray line, right axis). $D=0.02$ h^{-1}

transitions, the pigment composition profile remained almost the same.

MRPA values and photosynthetic parameters

Figure 5a represents $MRPA_{Cx}$ as a function of time during the two successive light step transitions. When the PFD increased from 75 to 765 µmol$_{photons}$ m^{-2}, $MRPA_{Cx}$ values instantly increased from 6 to 63 µmol$_{photons}$ g^{-1}$_{Cx}$ s^{-1}. These values of $MRPA_{Cx}$ were much higher than those obtained at steady-state, i.e., tenfold increase. It took about 100 h for $MRPA_{Cx}$ values to decrease and stabilize around 13 (± 1.0, $n=12$) µmol$_{photons}$ g^{-1}$_{Cx}$ s^{-1}. This decrease was the result of biomass concentration increase and cellular pigment content decrease. When the PFD decreased to 75 µmol$_{photons}$ m^{-2} s^{-1}, $MRPA_{Cx}$ values instantly decreased to 1.4 µmol$_{photons}$ g^{-1}$_{Cx}$ s^{-1}. Then $MRPA_{Cx}$ values increased again to reach, after about 150 h, the same values as at the beginning of the experiment. It should be noted that the stabilization time for $MRPA_{Cx}$ was the same as for biomass concentration or pigment concentration.

Microalgae are known to display different photoprotection and photoinhibition mechanisms to prevent damages caused by light stress. PAM chlorophyll *a* fluorescence was thus used to study the effect of PFD transitions on the dynamics of these mechanisms. Figure 5b gives the changes in F_v/F_m and *YNPQ* values during the two successive PFD steps. At the rising light step, F_v/F_m instantly decreased from 0.72 to 0.64 and stayed below 0.6 after 24 h. After about 150 h, F_v/F_m almost returned to its initial value. Then F_v/F_m progressively decreased over the next 300 h. When the light was set back to 75 µmol$_{photons}$ m^{-2} s^{-1}, F_v/F_m increased again after several hours to 0.72, and then slowly decreased over time to stabilize at 0.67.

During the whole experiment, *YNPQ* remained below 0.1. An increase was only observed at the beginning of the first light transition, corresponding to the largest MRPA values.

All these results indicate a different behavior between rising and falling steps. Both were investigated in details in the following sections.

Increasing light step

Figure 6a shows the evolution with time of the biomass concentration and the pigment content over the first 24 h after the rising light change. The biomass concentration increased immediately but the rate was low during the first 2 h, from 0.27 to 0.33 g L^{-1}. Then the increase became a little higher for the next 8 h, and biomass concentration reached 0.58 g L^{-1}. During the first 4 h, pigment content strongly decreased, from 8.4 to 5.8%$_{Cx}$. From 4 to 12 h, the rate was lower, from 5.8 to 4.5%$_{Cx}$. From the 12th hour, it must be noted that pigment content slowly increased (0.020%$_{Cx}$ h^{-1}).

Figure 6b shows the evolution with time of $MRPA_{Cx}$ values, resulting from biomass and pigment acclimation. As seen before, $MRPA_{Cx}$ instantly increased from 6 to 63 µmol$_{photons}$ g^{-1}_{Cx} s^{-1} just after the rising PFD step. Then it quickly decreased during the first 4 h, from 63 to 42 µmol$_{photons}$ g^{-1}_{Cx} s^{-1} and then the decrease slowed down to 30 µmol$_{photons}$ g^{-1}_{Cx} s^{-1} during the following 10 h. Interestingly, if the pigment specific $MRPA_{pig}$ is observed (Fig. 6c), it can be noticed that at the beginning of the light transition, after increasing, $MRPA_{pig}$ did not decrease and stayed constant around 0.74 ($\pm$0.01, n=5) µmol$_{photons}$ $mg^{-1}_{pigments}$ s^{-1} for 4 h.

Figure 6d shows photosynthetic parameters (i.e., F_v/F_m and *YNPQ* values) along the first 24 h after the rising step. As seen before, F_v/F_m decreased from 0.72 to 0.64. But this decrease was not instantaneous and took about 2 h. Just after the PFD change, *YNPQ* decreased from 0.07 to 0.00 and after 4 h, it started to increase to reach 0.09 after 12 h. However, 24 h after the light increase, *YNPQ* was almost equal to 0.00. It can be noted that the first decreases in F_v/F_m and in *YNPQ* have the same characteristic times, around 5 h.

Decreasing light step

Figure 7a shows the changes in biomass concentration and pigment content over time after the decrease in light from 765 to 75 µmol$_{photons}$ m^{-2} s^{-1}. During the very first hours after the light decrease, no evolution was clearly observed. The biomass concentration remained at the same level, at 1.31 ($\pm$0.01, n=5) g L^{-1} during the first 4 h, and then it decreased linearly to reach 0.65 g L^{-1} after 50 h (R^2=0.9924). This decrease in biomass concentration corresponds to a loss of 0.013 g L^{-1} h^{-1}, equal to 1% of initial concentration lost per hour. After 50 h, the decrease became slower (loss of 0.0045 g L^{-1} h^{-1}). Pigment content was almost constant during the first 12 h and stayed between 5.6 and 6.0%$_{Cx}$. Then, pigment content started to increase and reached 7.8%$_{Cx}$ after 100 h.

Figure 7b shows the evolution of $MRPA_{Cx}$ with time. The rate of photon absorption at compensation point (A_C) is also shown (A_C is equal to 2.8 µmol$_{photons}$ g^{-1}_{Cx} s^{-1} (Souliès et al. 2016)). Below this value, respiration prevailed over photosynthesis, resulting in a negative growth. This condition was observed just after the PFD decrease, where $MRPA_{Cx}$ decreased from 14.4 to 1.4 µmol$_{photons}$ g^{-1}_{Cx} s^{-1}. This value was found below A_C, so at this time, respiration should be

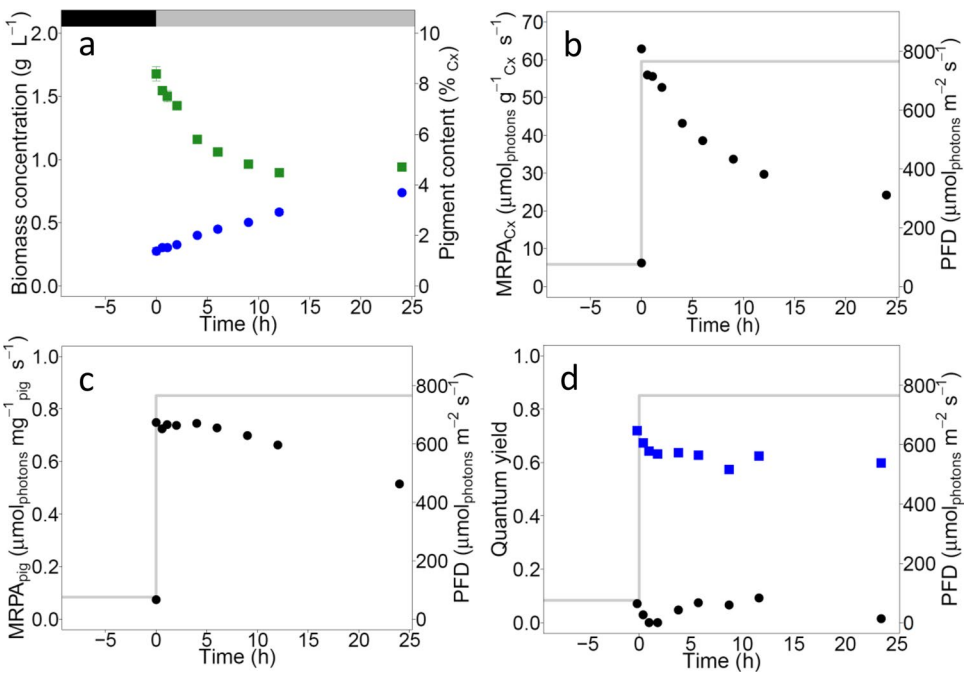

Fig. 6 Time response of *C. vulgaris* culture over time during the first 24 h of the increase in PFD from 75 to 765 µmol$_{photons}$ m^{-2} s^{-1}. D=0.02 h^{-1}. **a** shows biomass concentration (blue circles, left axis) and pigment content (green squares, right axis) changes with time. Black line represents 75 µmol$_{photons}$ m^{-2} s^{-1} and gray line represents 765 µmol$_{photons}$ m^{-2} s^{-1}. **b** shows the evolution of the biomass specific $MRPA_{Cx}$ with time (black circles, left axis). **c** shows the evolution of the pigment specific $MRPA_{pig}$ (black circles, left axis). **d** shows changes in F_v/F_m (blue squares) and *YNPQ* (black circles, left axis) with time. In **b**, **c**, and **d**, the gray line (right axis) represents the PFD. Error bars represent standard deviation (n=3)

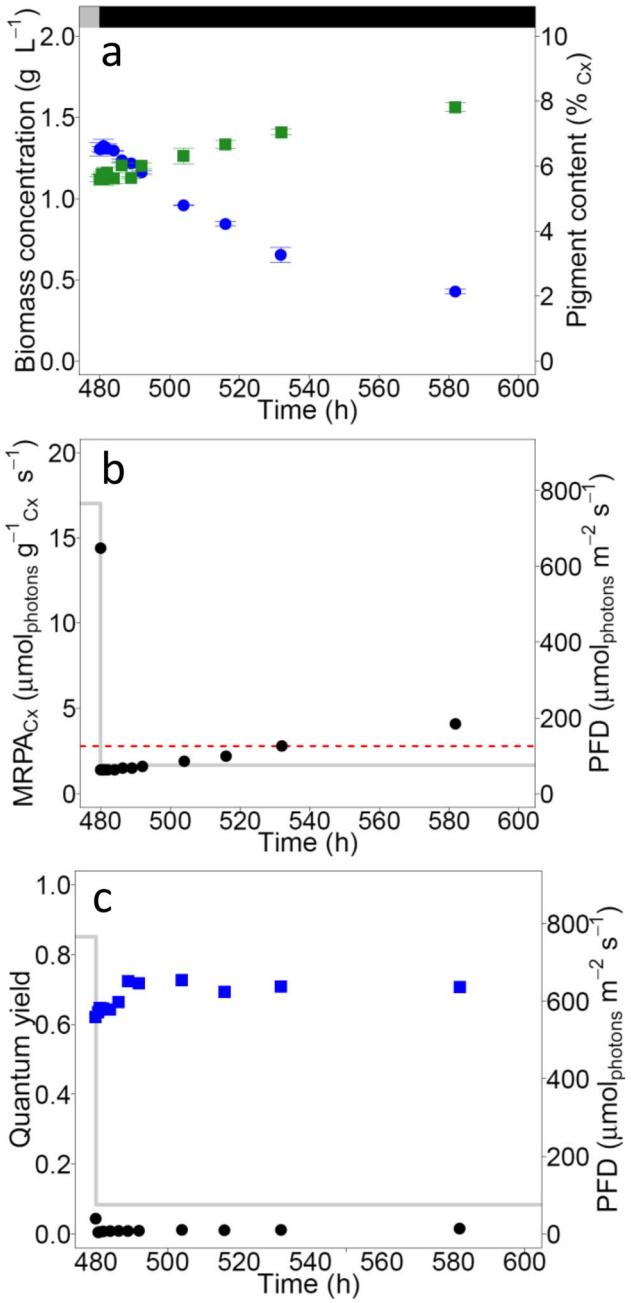

Fig. 7 Time response of *C. vulgaris* culture over time during the first 120 h after a PFD step from 765 to 75µmol$_{photons}$ m^{-2} s^{-1}. $D = 0.02$ h^{-1}. **a** shows the changes in biomass concentration (blue circles, left axis) and pigment content (green squares, right axis) with time. Black line represents 75 µmol$_{photons}$ m^{-2} s^{-1} and gray line represents 765 µmol$_{photons}$ m^{-2} s^{-1}. **b** shows the biomass specific $MRPA_{Cx}$ (black circles, left axis). **c** shows the changes in F_v/F_m (blue squares) and *YNPQ* (black circles, left axis) with time. In **b** and **c**, the gray line (right axis) represents the PFD. Error bars represent standard deviation ($n = 3$)

predominant. $MRPA_{Cx}$ stayed at this same level for 6 h. Then it started to increase and reached A_C value, 50 h after the light decrease. $MRPA_{Cx}$ stabilized around 5 µmol$_{photons}$ g^{-1}$_{Cx}$ s^{-1} after 150 h at the new PFD level.

Figure 7c shows the evolution with time of F_v/F_m and *YNPQ*. When the incident light decreased, F_v/F_m took 8 h to reach a maximal value, from 0.62 to 0.72. Then it remained almost stable. *YNPQ* instantly decreased from 0.04 to 0.00 after the light change, and it stayed unchanged during the whole experiment.

Discussion

MRPA correlates changes in light received with biomass and pigment concentration evolutions

A decreasing relationship, with two successive linear relations, was found between total pigment content and MRPA for *Chlorella vulgaris* culture obtained in continuous light (Fig. 3). Those correlations were found valid whatever the light attenuation profile, as concentrated cultures (illumination fraction equal to 0.40) led to the same result as diluted cultures (transmittance equal to 0.43). Both light regimes inside the culture volumes were very different. Indeed a γ equal to 0.40 means that more than half of the culture volume was not illuminated. And a T equal to 0.43 means that all the culture volume was illuminated, and almost half of the incident PFD reached the bottom of the culture. This could be considered a surprising observation because having or not a dark volume in a PBR is well known to result in very different kinetic performances (e.g., averaged growth rate) of the microalgae culture (Takache et al. 2012; Acien et al. 2013). In this study, the light attenuation profile (with or without dark volume) did not affect the pigment content in *C. vulgaris*. Only the averaged MRPA was found to have an influence.

Moreover, the fact that the pigment content almost remained stable at values of ca. 4%$_{Cx}$ suggested that this could be the minimal total pigment content that can be obtained in *C. vulgaris* when cultivated in nutrient-enriched conditions and continuous light.

Under dynamic light conditions, MRPA values had an amplitude larger than under continuous light conditions. Very high $MRPA_{Cx}$ values were then transitory observed (> 50 µmol$_{photon}$ g^{-1}$_{Cx}$ s^{-1}) similar to those encountered in solar cultures due to high light fluctuations (Pruvost et al., 2017). During the PFD light steps, time evolutions of biomass concentration, pigment content, and $MRPA_{Cx}$ were closely related. In both light transitions, the same stabilization times were observed for these parameters (around 150 h). Moreover, at the beginning of the rising light transition, a similar evolution of pigment content and $MRPA_{Cx}$

was observed, with a decrease of both parameters. This can be explained by the decrease in pigment content leading to a decrease in the capacity of light absorption by cells. As a consequence, less photons were absorbed for the same biomass concentration. Considering $MRPA_{pig}$ instead of the $MRPA_{Cx}$, it remained unchanged for a few hours after the light increase. This illustrates the relation between MRPA and the pigment changes during photoacclimation, as already observed in continuous light with the linear evolution between MRPA and pigment content. Under the studied dynamic light conditions, a large variation of MRPA values was obtained, reflecting pigment content evolutions. When expressing MRPA values as a function of pigment content ($MRPA_{pig}$), it tends to reduce its variation in contrast to values determined as a function of biomass concentration.

All these results tend to indicate a universal relation between MRPA and pigment content values when *C. vulgaris* is cultivated in continuous light. And when a light step transition is applied, MRPA values are suddenly modified and the culture metabolism becomes unbalanced. From this point, both the biomass concentration and the pigment content evolve to reach a new steady-state, in which the relation between MRPA and pigment content achieved at steady-state in continuous light is again verified.

As already suggested in a previous study (Pruvost et al., 2017), MRPA thus reveals an interesting integrative parameter in microalgal culture systems as it enables to relate various quantities such as biomass concentration, pigment content (i.e., radiative properties), PFD, and PBR design (i.e., culture depth). Indeed, the present study shows that MRPA values both reflect the efficiency of light absorption due to the pigment content in *C. vulgaris* and the light attenuation conditions in the PBR. The former because it is a cell characteristic that changes with the microalga photoacclimation state, the latter because it is a consequence of this phenomenon and of cell density. In fact, this demonstrates the reliability of the MRPA parameter to pinpoint the tight coupling between PFD, biomass and pigment concentration, and metabolism.

Difference in dynamics between MRPA and microalgae biomass and pigment concentration

In both PFD transitions (high to low vs. low to high), MRPA values instantly changed after the light change. However, the resulting changes in biomass concentration and pigment content remained slower. In the rising light transition, the pigment content decreased very rapidly but this decrease was probably accentuated by the dilution rate and biomass increase was slow during the few first hours. After the PFD decrease, both biomass concentration and pigment content remained at the same values for a few hours. In both transitions, biomass concentration and pigment content took more than 100 h to stabilize.

Note that the increase in biomass concentration took longer than its decrease. This could be explained by the fact that in continuous chemostat cultures, a dilution rate is applied. As a consequence, to have a marked increase in the biomass concentration in such systems, a large increase in the biosynthesis rate is required and the energetic demand for this increase is high.

In both transitions, pigment content was found to stabilize faster than biomass concentration. In our case, the lowest value of pigment content was reached 10 h after the first light change, which was very fast compared to biomass evolution (more than 200 h to reach steady-state value). This is certainly explained by the global effect on light attenuation conditions: because biomass concentration increased with PFD, the light received into the PBR (i.e., the MRPA) decreased progressively and the pigment content increased again. When considering the PFD decrease, a progressive evolution toward steady-state values was also observed but, because of the need to synthetize de novo pigments, the dynamics was slower.

Contrary to biomass and pigment dynamics, parameters related to photosynthesis and MRPA responded quickly after both PFD transitions. Indeed, F_v/F_m and *YNPQ* decreased a few minutes just after the light increase. This transient slowdown of the photosynthesis efficiency is moderate and it could illustrate the capacity of *C. vulgaris* to rapidly quench energy in excess using state transition, a process different from photochemistry and other NPQ components (heat dissipation, photoinhibition). Indeed, green algae are known to adjust the absorption of light energy by both photosystems PSII and PSI, by transfer of mobile components of their light harvesting complexes (LHC) (e.g., Allen and Forsberg 2001; Goldschmidt-Clermont and Bassi 2015). This process dissipates in minutes (Muller et al. 2001). On the longer term, *YNPQ* increased again after a few hours. A few minutes after the opposite light step transition, *YNPQ* decreased and YPSII started to increase.

In summary, our study showed that a sudden transition in MRPA is associated to slow responses of biomass concentration and pigment content (characteristic times in the range of hours). But, on the other hand, it was observed a rapid time response of parameters related to photosynthesis. From this, it is deduced that rising and falling MRPA values dynamically reflect the direct impacts of light changes on the early photosynthetic events (PSII quantum yield and electron transport chain), and that it takes more time for the whole metabolism to respond and adapt to these light changes. This is in the line of previous observations on the diversity in short-term and a long-term photoacclimation phenomena (Brunet et al. 2011).

We can also note that the time to reach a steady-state was higher to 1 day after both transitions. As a consequence, in actual day-night cycles, microalgae will never have enough time to reach steady-state. In such conditions, cells and culture can be always considered in a transitory regime. This point deserves special consideration when designing and operating PBRs on the long term.

Different biological mechanisms involved when increasing and decreasing PFD transitions

Increasing and decreasing incident lights were shown to lead to different response times. This can be explained by the different photosynthetic mechanisms involved during these transitions.

When PFD increased, the main parameters that changed were F_v/F_m and *YNPQ*. A decrease in F_v/F_m was observed and it became below 0.7. It can be a sign of photoinhibition (Malapascua et al., 2014) which corresponds to a damage of the photosynthetic apparatus leading to a decrease in the photosynthesis efficiency (Kok 1956; Nixon et al. 2010). So as long as F_v/F_m was low, microalgae were not able to use light with the best efficiency to grow. F_v/F_m reached its initial value at the same time as pigment content stabilized. This supposes that photoacclimation processes allowed cells to recover from photoinhibition.

In parallel, after the light increase, when *YNPQ* values became a little higher, biomass concentration started to increase at a higher rate and the pigment content decrease at a lower rate. *YNPQ* was never high but in this experiment, considering light attenuation, the maximal mean fluence rate was about 300 $\mu mol_{photons}\ m^{-2}\ s^{-1}$. At this level, photoprotection is known to remain low in *C. vulgaris* (Malapascua et al. 2018; Bonnanfant et al. 2019). Thus, even being low, *YNPQ* might have played a role in photoprotection during the first few hours after the light increase.

Note that during the rising PFD transition, the chlorophyll *a* to carotenoids ratio was constant, indicating no marked light stress, which should have induced an increase in carotenoid relative concentration, a well-known effect of light stress response in *C. vulgaris* (Dubinsky and Stambler 2009; Sharma 2012). In our study, the light level applied was probably not high enough to induce the production of carotenoids known to protect the cells against the oxidative stress (Ortega-Villasante et al. 2016).

The mechanisms involved in the decreasing PFD transition were not the same as the ones observed in the opposite light transition. Here, the photoacclimation response was mainly due to the limitation of light in the PBR. Indeed, when the PFD decreased, MRPA value was below A_C so the culture was light limited and respiration was predominant. As a consequence, biomass concentration decreased at a high rate, which, in turn, resulted in an increase in light availability for cells (increase in MRPA). From this point, F_v/F_m reached its maximum value, reflecting the fact that microalgae photoacclimated to the new light conditions, so they were able to use light with the best efficiency. As a consequence, the decrease in biomass concentration slowed down.

To conclude, for the two light acclimation phases (high to low vs. low to high), photosynthetic mechanisms involved were not the same. When incident light increased, *YNPQ* was transiently low, indicating that photoprotection only played a small role, whereas it remained close to zero when light decreased. F_v/F_m decreased instantly when light increased but it took several hours to increase again after PFD decreased. So under a rising light, photoinhibition occurred almost instantly and then photoprotection mechanisms were established for some hours; however, after decreasing light, no photoprotection was observed and the light received by the cells was probably too low for the photosystem to adjust quickly and to reach immediately an optimal photochemical yield.

Whatever the case, MRPA was found a very valuable parameter to relate light received by cells (as affected by changes in PFD, but also biomass and pigment concentrations) and corresponding biological responses. After each light change, several biological mechanisms took place and fine-tuned to let microalgae acclimate to the new conditions, both on the short term and on the long term. A rising PFD step to high irradiance trigger photoinhibition and photoprotection mechanisms whereas after a decreasing PFD step, cells do not rely on photoprotection to photoacclimate to low irradiance, and the culture was light limited for a few hours. Consequently, the response times for photoacclimation were not the same between these opposite transitions. However, the time for biomass concentration and pigment content to stabilize was always superior to 100 h. This again confirms that in the actual conditions of a solar production with day/night cycles, similarly to any photosynthetic organisms growing outdoor, *C. vulgaris* cultures will always be in a transitory regime with regards to their photosynthetic and metabolic responses.

As a result, the study of the dynamic mechanisms which intervene in the response of microalgae in variable light conditions is therefore essential for the good understanding and control of solar culture systems. Future studies will aim to extend the approaches developed here in real solar conditions, in particular taking into account UV damaging effects. Other biological models will also be studied to see how changes in quantities linked to the adaptive capacity of cells (as for example NPQ level and its kinetics of evolution toward light change) play on growth performance in solar culture conditions.

Acknowledgements We are very grateful to the AMI (Atlantic MIcroalgae) scientific consortium and the Pays de la Loire region (France), who have supported our research. MB also benefitted from a training on fluorescence techniques in the laboratory of Dr. D. Campbell (Mount Allison University, Canada).

Author contribution JP and MB conceived and designed research. MB conducted experiments. HM contributed to the conception and design of the experimental setups. JP and MB analyzed data. MB wrote the manuscript. All authors read, reviewed, and approved the manuscript.

Funding The work was partly funded by the AMI (Atlantic MIcroalgae) project and the Pays de la Loire region (France). The European Commission Horizon 2020 Research and Innovation Program GHaNA, The Genus Haslea, New marine resources for blue biotechnology and Aquaculture, grant agreement No [734708/GHANA/H2020-MSCA-RISE-2016] funded the training of MB in the laboratory of Dr. D. Campbell (Mount Allison University, Canada).

Data availability All data are available on simple request.

Code availability Not applicable.

Declarations

Consent to participate We state that no conflicts, informed consent, human or animal rights applicable.

Consent for publication We hereby state that all authors mutually agree that it should be submitted for publication and that it is our original work. The manuscript has been read and approved by all named authors and that there are no other persons who satisfied the criteria for authorship but are not listed. We further confirm that the order of authors listed in the manuscript has been approved by all of us.

References

Acien G, Fernandez-Sevilla JM, Molina-Grima E (2013) Photobioreactors for the production of microalgae. Reviews in Environ Sci and Bio/Technol 12. https://doi.org/10.1007/s11157-012-9307-6

Allen J, Forsberg J (2001) Allen, J. F. & Forsberg, J. Molecular recognition in thylakoid structure and function. Trends Plant Sci 6:317–326. https://doi.org/10.1016/S1360-1385(01)02010-6

Andersen RA (2005) Algal culturing techniques - 1st edition. https://www.elsevier.com/books/algal-culturing-techniques/andersen/978-0-12-088426-1. Accessed 14 Feb 2019

Asada K (2000) The water-water cycle as alternative photon and electron sinks. Philos Trans R Soc Lond B Biol Sci 355:1419–1431

Bennoun P (1982) Evidence for a respiratory chain in the chloroplast. Proc Natl Acad Sci U S A 79:4352–4356

Bonnanfant M, Jesus B, Pruvost J, Mouget J-L, Campbell DA (2019) Photosynthetic electron transport transients in *Chlorella vulgaris* under fluctuating light. Algal Res 44:101713. https://doi.org/10.1016/j.algal.2019.101713

Brunet C, Johnsen G, Lavaud J, Roy S (2011) Pigments and photoacclimation processes. In: Phytoplankton pigments: characterization, chemotaxonomy and applications in oceanography

Crofts AR, Wraight CA (1983) The electrochemical domain of photosynthesis. Biochimica et Biophysica Acta (BBA) - Reviews on Bioenergetics 726:149–185. https://doi.org/10.1016/0304-4173(83)90004-6

Degrenne B, Pruvost J, Christophe G, Cornet JF, Cogne G, Legrand J (2010) Investigation of the combined effects of acetate and photobioreactor illuminated fraction in the induction of anoxia for hydrogen production by *Chlamydomonas reinhardtii*. Int J Hydrogen Energy 35:10741–10749. https://doi.org/10.1016/j.ijhydene.2010.02.067

Dubinsky Z, Stambler N (2009) Photoacclimation processes in phytoplankton: mechanisms, consequences, and applications. Aquat Microb Ecolog 56:163–176. https://doi.org/10.3354/ame01345

Goldschmidt-Clermont M, Bassi R (2015) Sharing light between two photosystems: mechanism of state transitions. Curr Opin Plant Biol 25:71–78. https://doi.org/10.1016/j.pbi.2015.04.009

Goss R, Lepetit B (2015) Biodiversity of NPQ. J Plant Physiol 172:13–32. https://doi.org/10.1016/j.jplph.2014.03.004

Heinz Walz GmbH (2001) Instruction manual for PAM-CONTROL

Ifrim GA, Titica M, Cogne G, Boillereaux L, Legrand J, Caraman S (2014) Dynamic pH model for autotrophic growth of microalgae in photobioreactor: a tool for monitoring and control purposes. AIChE J 60:585–599. https://doi.org/10.1002/aic.14290

Kandilian R, Pruvost J, Artu A, Lemasson C, Legrand J, Pilon L (2016) Comparison of experimentally and theoretically determined radiation characteristics of photosynthetic microorganisms. J Quant Spectrosc Radiat Transfer 175:30–45. https://doi.org/10.1016/j.jqsrt.2016.01.031

Kargul J, Barber J (2008) Photosynthetic acclimation: structural reorganisation of light harvesting antenna – role of redox-dependent phosphorylation of major and minor chlorophyll a/b binding proteins. FEBS J 275:1056–1068. https://doi.org/10.1111/j.1742-4658.2008.06262.x

Kazbar A, Cogne G, Urbain B, Marec H, Le-Gouic B, Tallec J, Takache H, Ismail A, Pruvost J (2019a) Effect of dissolved oxygen concentration on microalgal culture in photobioreactors. Algal Research 101. https://doi.org/10.1016/j.algal.2019.101432

Kazbar A, Marec H, Takache H, Ismail A, Pruvost J (2019b) Effect of design dark fraction on the loss of biomass productivities in photobioreactors. Bioprocess Biosyst Eng. https://doi.org/10.1007/s00449-019-02217-3

Klughammer C, Schreiber U (2008) Complementary PS II quantum yields calculated from simple fluorescence parameters measured by PAM fluorometry and the saturation pulse method. PAM Application Notes 1:27–35

Kok B (1956) On the inhibition of photosynthesis by intense light. Biochimica Biophysica Acta 21:234–244. https://doi.org/10.1016/0006-3002(56)90003-8

Kolber Z, Falkowski PG (1993) Use of active fluorescence to estimate phytoplankton photosynthesis in situ. Limnol Oceanogr 38:1646–1665. https://doi.org/10.4319/lo.1993.38.8.1646

Lavaud J (2007) Fast regulation of photosynthesis in diatoms: mechanisms, evolution and ecophysiology. Func Plant Sci Biotech 1:267–287

Le Borgne F (2011) Développement d'un photobioréacteur solaire intensifié en vue de la production à grande échelle de biomasse microalgale. Thesis, Nantes

Le Gouic B, Marec H, Pruvost J, Cornet J-F (2021) Investigation of growth limitation by CO_2 mass transfer and inorganic carbon source for the microalga *Chlorella vulgaris* in a dedicated photobioreactor. Chem Eng Sci (in press)

Malapascua JRF, Jerez CG, Sergejevová M, Figueroa FL, Masojídek J (2014) Photosynthesis monitoring to optimize growth of microalgal mass cultures: application of chlorophyll fluorescence techniques. Aquat Bio 22:123–140. https://doi.org/10.3354/ab00597

Malapascua JRF, Ranglova K, Masojidek J (2018) Photosynthesis and growth kinetics of *Chlorella vulgaris R-117* cultured in an internally LED-illuminated photobioreactor. Photosynthetica. https://doi.org/10.32615/ps.2019.031

Muller P, Li X, Niyogi KK (2001) Non-photochemical quenching. A response to excess light energy. Plant Physiol 125:1558–1566

Nixon PJ, Michoux F, Yu J, Boehm M, Komenda J (2010) Recent advances in understanding the assembly and repair of photosystem II. Ann Bot 106:1–16. https://doi.org/10.1093/aob/mcq059

Ortega-Villasante C, Burén S, Barón-Sola Á, Martínez F, Hernández LE (2016) In vivo ROS and redox potential fluorescent detection in plants: present approaches and future perspectives. Methods 109:92–104. https://doi.org/10.1016/j.ymeth.2016.07.009

Peltier G, Cournac L (2002) Chlororespiration Annual Rev Plant Bio 53:523–550. https://doi.org/10.1146/annurev.arplant.53.100301.135242

Perkins RG, Kromkamp JC, Serôdio J, Lavaud J, Jesus B, Mouget J-L, Lefebvre S, Forster RM (2010) The application of variable chlorophyll fluorescenceto microphytobenthic biofilms. In: Chlorophyll a fluorescence in aquatic sciences: methods and applications

Pottier L, Pruvost J, Deremetz J, Cornet J-F, Legrand J, Dussap CG (2005) A fully predictive model for one-dimensional light attenuation by *Chlamydomonas reinhardtii* in a torus photobioreactor. Biotechnol Bioeng 91:569–582. https://doi.org/10.1002/bit.20475

Prasil O, Kolber Z, Berry JA, Falkowski PG (1996) Cyclic electron flow around photosystem II in vivo. Photosynth Res 48:395–410. https://doi.org/10.1007/BF00029472

Pruvost J, Cornet JF (2012) Knowledge models for engineering and optimization of photobioreactors. In: C.Walter CPa (ed) Microalgal biotechnology. De Gruyter GmbH & Co. KG, pp 181–224

Pruvost J, Cornet JF, Le Borgne F, Goetz V, Legrand J (2015) Theoretical investigation of microalgae culture in the light changing conditions of solar photobioreactor production and comparison with cyanobacteria. Algal Res 10:87–99. https://doi.org/10.1016/j.algal.2015.04.005

Pruvost J, Cornet J-F, Legrand J (2008) Hydrodynamics influence on light conversion in photobioreactors: an energetically consistent analysis. Chem Eng Sci 63:3679–3694. https://doi.org/10.1016/j.ces.2008.04.026

Pruvost J, Le Borgne A, Artu A, Legrand J (2017) Development of a thin-film solar photobioreactor with high biomass volumetric productivity (AlgoFilm) based on process intensification principles. Algal Research 21:120–137. https://doi.org/10.1016/j.algal.2016.10.012

Pruvost J, Le Borgne F, Cornet J-F, Legrand J (2016) Chapter five - industrial photobioreactors and scale-up concepts. In: Legrand J (ed) Adv Chem Eng. Academic Press, pp 257–310

Pruvost J, Pottier L, Legrand J (2006) Numerical investigation of hydrodynamic and mixing conditions in a torus photobioreactor. Chem Eng Sci 61:4476–4489. https://doi.org/10.1016/j.ces.2006.02.027

Richmond A (2013) Biological principles of mass cultivation of photoautotrophic microalgae. In: Handbook of microalgal culture. John Wiley & Sons, Ltd, pp 169–204

Ritchie RJ (2008) Universal chlorophyll equations for estimating chlorophylls a, b, c, and d and total chlorophylls in natural assemblages of photosynthetic organisms using acetone, methanol, or ethanol solvents. Photosynthetica 46:115–126. https://doi.org/10.1007/s11099-008-0019-7

Sharma R (2012) Effects of culture conditions on growth and biochemical profile of *Chlorella vulgaris*. J Plant Pathol Microbiol 03. https://doi.org/10.4172/2157-7471.1000131

Souliès A, Legrand J, Marec H, Pruvost J, Castelain C, Burghelea T, Cornet J-F (2016) Investigation and modeling of the effects of light spectrum and incident angle on the growth of *Chlorella vulgaris* in photobioreactors. Biotechnol Prog 32:247–261. https://doi.org/10.1002/btpr.2244

Strickland JDH, Parsons TR (1968) A practical handbook of seawater analysis. Fisheries Research Board of Canada

Sueoka N (1960) Mitotic replication of deoxyribonucleic acid in *Chlamydomonas reinhardii*. Proc Natl Acad Sci U S A 46:83–91

Takache H, Pruvost J, Cornet J-F (2012) Kinetic modeling of the photosynthetic growth of *Chlamydomonas reinhardtii* in a photobioreactor. Biotechnol Prog 28:681–692. https://doi.org/10.1002/btpr.1545

Takache H, Pruvost J, Marec H (2015) Investigation of light/dark cycles effects on the photosynthetic growth of *Chlamydomonas reinhardtii* in conditions representative of photobioreactor cultivation. Algal Res 8:192–204. https://doi.org/10.1016/j.algal.2015.02.009

Titica M, Kazbar A, Marec H, Pruvost J, Ifrim george, barbu marian, Caraman S (2018) Simultaneous control of pH and dissolved oxygen in closed photobioreactor. In: 2018 22nd international conference on system theory, control and computing (ICSTCC). IEEE, Sinaia, France, pp 372–378